Acta Crystallographica Section A
Foundations of Crystallography
ISSN 0108-7673

Received 21 March 2000
Accepted 3 May 2000

The phenomenon of polarization suppression of X-ray *Umweg* multiple waves in crystals

Yuri P. Stetsko,[a,d]* Hellmut J. Juretschke,[c] Yi-Shan Huang,[a] Chun-Hsiung Chao,[a] Chun-Kuang Chen[a] and Shih-Lin Chang[a,b]

[a]Department of Physics, National Tsing Hua University, Hsinchu, Taiwan 300, [b]Synchrotron Radiation Research Center, Hsinchu, Taiwan 300, [c]Department of Physics, Polytechnic University, Brooklyn, New York 11201, USA, and [d]Chernovtsy State University, Chernovtsy 274012, Ukraine. Correspondence e-mail: stetsko@phys.nthu.edu.tw

The phenomenon of the polarization suppression of X-ray *Umweg* multiple waves in Renninger scans [Renninger (1937). *Z. Kristallogr.* **97**, 107–121] of crystals, showing intensity decrease due to properly chosen wavelength and polarization of incident radiation, is observed. That is, one of the participating wave components in the multiple-wave interference is reduced considerably so that the intensity of multiple diffraction is decreased. The condition for total suppression of the multiple-wave interaction in crystals is derived theoretically from the Born approximation and verified with exact dynamical calculation and experiments. Partial suppression of the strong *Umweg* interfered component is demonstrated using elliptically or linearly polarized synchrotron radiation. The suppressed multiple-wave intensity distribution reveals high sensitivity to X-ray reflection phase. This multiple-diffraction technique under partial polarization suppression provides an alternative way of enhancing the visibility of multiple-wave interference in crystals for direct phase determination.

1. Introduction

Phase determination is a long-standing problem in diffraction physics and X-ray crystallography (Hauptman, 1989). Because the measured intensity of Bragg diffraction is proportional to the product of the structure factor and its complex conjugate, the phase of the structure factor is lost. This phase is an indispensable piece of information for determining the relative positions of atoms in a crystal unit cell, namely the crystal structure. Several solutions to the phase problem have been developed: direct methods, which utilize a large collection of diffraction data (Schenk, 1991); multiwavelength anomalous dispersion, which utilizes resonance scattering (Hendrickson, 1991); and many others (Woolfson & Fan, 1995). Very recently, multiple-wave diffraction has demonstrated its capability of determining the phases of the involved structure-factor multiplets (Chang, 1987, 1998; Weckert & Hümmer, 1997, and references therein) utilizing the coherent dynamical interaction among the multiply diffracted waves. In this way, the phases of individual Bragg reflections can be deduced (Chang, 1984) from the determined multiplets, thus providing a solution to the X-ray phase problem. However, there is a fundamental concern in the visibility of X-ray multiple-wave interaction in crystals, which is also very common in optics. That is, the visibility of the interference effect is low when the amplitudes of the involved multiply diffracted waves are not comparable with each other. In other words, the phase-insensitive part of the diffracted intensities plays a dominant role in the diffraction process. Under this circumstance, the determined phase values may not be reliable. In the literature, Weckert & Hümmer (1997) have pointed out that the required interference visibility for correct phase determination can be achieved by choosing proper reflections of comparable structure-factor amplitudes. Shen & Finkelstein (1990) also mentioned that use of an elliptically polarized beam could increase the multiple-wave interference effect due to the changing of the peak-profile asymmetry. In this paper, we propose an alternative way of enhancing the interference visibility, namely the phase sensitivity, by suppressing the phase-insensitive contribution to a minimum using a properly chosen wavelength and linear polarization of incident radiation. It is demonstrated that partial polarization suppression with a linearly polarized incident wave, as well as total suppression with a slightly elliptically polarized incident wave, could enhance the interference visibility in multiple diffraction and thus provide reliable phase information.

2. Polarization suppression

2.1. Theoretical consideration

Multiple diffraction takes place when more than one set of atomic planes is simultaneously brought into position to diffract an incident beam. Experimentally (Renninger, 1937), to generate a three-wave (O, G, L) diffraction, the crystal is first aligned for the G reflection (the primary reflection) for an

incident wave O and is then rotated (the azimuthal ψ scan) around the reciprocal-lattice vector $\mathbf{G}$ of the G reflection to satisfy Bragg's law for the secondary reflection L, without disturbing the primary reflection. The interaction among the G and L reflections *via* the $G-L$ coupling usually modifies the intensity of the primary as well as the secondary reflection. This intensity modification can be accounted for using numerical calculations based on the dynamical theory (Colella, 1974; Chang, 1984; Stetsko & Chang, 1997), the Takagi–Taupin equations (for example, Thorkildsen, 1987; Thorkildsen & Larsen, 1998; Larsen & Thorkildsen, 1998), the Bethe approximation (Juretschke, 1982*a*,*b*, 1984, 1998; Høier & Marthinsen, 1983; Hümmer & Billy, 1986; Chang, Stetsko *et al.*, 1999) and the Born approximation (Shen, 1986, 1998; Shen & Colella, 1988; Chang & Tang, 1988; Chang *et al.*, 1989; Shen & Finkelstein, 1990, 1992; Shen *et al.*, 1995).

In the second-order Born approximation, the wavefield $\mathbf{D}_{G(3)}$ of a three-wave (O, G, L) case depends on the interaction of the wavefield $\mathbf{D}_{G(2)}$ of the two-wave (O, G) diffraction and the field $\mathbf{D}_{G(um)}$ of the *Umweg* (detoured) diffraction. The latter involves the consecutive reflections first by the L reflection and then by the coupling reflection $G-L$, so that the diffracted wave is along the same direction as that of the primary reflection. Hence,

$$\begin{aligned}\mathbf{D}_{G(3)} &= \mathbf{D}_{G(2)} + \mathbf{D}_{G(um)} \\ &= A_G \mathbf{s}_G \times \mathbf{s}_G \times [\chi_G \mathbf{D}_O + A_L \chi_{G-L} \chi_L \mathbf{s}_L \times (\mathbf{s}_L \times \mathbf{D}_O)],\end{aligned} \tag{1}$$

where $\mathbf{D}_O$ is the incident wavefield with magnitude D_O and the resonance term $A_H = K_H^2/[k^2 - K_H^2(1-\chi_O)]$ with $H = G, L$. Here, $k = 1/\lambda$ and K_H are the magnitudes of the wavevectors in vacuum and inside the crystal, respectively, and $\mathbf{s}_H$ are the unit vectors of the diffracted waves; $\chi_H = \Gamma F_H$ is the Fourier component of the crystal polarizability for $H = O, G, L, G-L$, F_H is the structure factor of the H reflection, $\Gamma = -r_e\lambda^2/\pi V$, where r_e is the classical radius of the electron, λ is the incident X-ray wavelength and V is the unit-cell volume.

Suppose that the direction of polarization of a linearly polarized incident wave $\mathbf{D}_O = D_O \mathbf{p}_O$ is along an arbitrary unit vector $\mathbf{p}_O$ denoted as $\mathbf{p}_O = \alpha\boldsymbol{\sigma} + \beta\boldsymbol{\pi}_O$, where the polarization unit vectors are defined as $\boldsymbol{\sigma} \equiv \boldsymbol{\sigma}_O = -[\mathbf{s}_O \times \mathbf{s}_G]/|[\mathbf{s}_O \times \mathbf{s}_G]|$ and $\boldsymbol{\pi}_O = [\mathbf{s}_O \times \boldsymbol{\sigma}]$, $\mathbf{s}_O$ is the unit vector of the incident wave. Hence, $\alpha = \cos\omega$ and $\beta = \sin\omega$, where ω is the angle between $\mathbf{p}_O$ and the $\boldsymbol{\sigma}$ vector (see Fig. 1). From equation (1), the fields

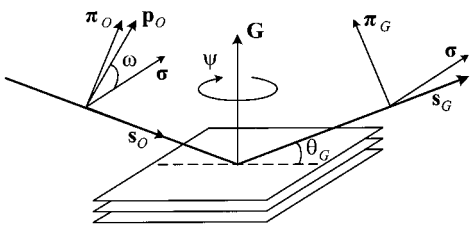

Figure 1
Definition of the polarization unit vectors in two-wave diffraction.

$\mathbf{D}_{G(2)}$ and $\mathbf{D}_{G(um)}$ for cases involving incident radiation far from the absorption edges of the constituent atoms of the crystal take the form (see also Shen & Finkelstein, 1992; Shen *et al.*, 1995)

$$\mathbf{D}_{G(2)}(\mathbf{p}_O) = A_G \chi_G \mathbf{p}_{G(2)}(\mathbf{p}_O) D_O, \tag{2a}$$

$$\mathbf{D}_{G(um)}(\mathbf{p}_O) = A_G A_L \chi_{G-L} \chi_L \mathbf{p}_{G(um)}(\mathbf{p}_O) D_O, \tag{2b}$$

where

$$\mathbf{p}_{G(2)}(\mathbf{p}_O) = (\alpha P_G^\sigma \boldsymbol{\sigma} + \beta P_G^\pi \boldsymbol{\pi}_G), \tag{3a}$$

$$\mathbf{p}_{G(um)}(\mathbf{p}_O) = [p_{um}^\sigma(\mathbf{p}_O)\boldsymbol{\sigma} + p_{um}^\pi(\mathbf{p}_O)\boldsymbol{\pi}_G] \tag{3b}$$

are the polarization vectors respectively of the two-wave reflection G and the *Umweg* wave represented in coordinate system $(\boldsymbol{\sigma}, \boldsymbol{\pi}_G)$, where the polarization unit vector $\boldsymbol{\pi}_G = [\mathbf{s}_G \times \boldsymbol{\sigma}]$ (see Fig. 1). $P_G^\sigma = 1$ and $P_G^\pi = \cos 2\theta_G$ are the polarization factors of the two-wave reflection G, where θ_G is the Bragg angle. The polarization factors $p_{um}^\sigma(\mathbf{p}_O)$ and $p_{um}^\pi(\mathbf{p}_O)$ of the *Umweg* wave for arbitrary polarization vector $\mathbf{p}_O$ of the incident wave are expressed as

$$p_{um}^\sigma(\mathbf{p}_O) = \alpha p_{um}^\sigma(\boldsymbol{\sigma}) + \beta p_{um}^\sigma(\boldsymbol{\pi}_O), \tag{4a}$$

$$p_{um}^\pi(\mathbf{p}_O) = \alpha p_{um}^\pi(\boldsymbol{\sigma}) + \beta p_{um}^\pi(\boldsymbol{\pi}_O), \tag{4b}$$

in terms of the polarization factors $p_{um}^\sigma(\boldsymbol{\sigma})$ and $p_{um}^\pi(\boldsymbol{\sigma})$ for the σ-polarized incident radiation,

$$p_{um}^\sigma(\boldsymbol{\sigma}) = P_G^\sigma - (\boldsymbol{\sigma} \cdot \mathbf{s}_L)^2 \tag{5a}$$

$$p_{um}^\pi(\boldsymbol{\sigma}) = -(\boldsymbol{\sigma} \cdot \mathbf{s}_L)(\boldsymbol{\pi}_G \cdot \mathbf{s}_L), \tag{5b}$$

and the polarization factors $p_{um}^\sigma(\boldsymbol{\pi}_O)$ and $p_{um}^\pi(\boldsymbol{\pi}_O)$ for the π-polarized incident radiation,

$$p_{um}^\sigma(\boldsymbol{\pi}_O) = -(\boldsymbol{\sigma} \cdot \mathbf{s}_L)(\boldsymbol{\pi}_O \cdot \mathbf{s}_L) \tag{6a}$$

$$p_{um}^\pi(\boldsymbol{\pi}_O) = P_G^\pi - (\boldsymbol{\pi}_O \cdot \mathbf{s}_L)(\boldsymbol{\pi}_G \cdot \mathbf{s}_L) \tag{6b}$$

(see also Shen & Finkelstein, 1992; Shen *et al.*, 1995; Stetsko & Chang, 1999*b*).

When the amplitudes of $\mathbf{D}_{G(2)}$ and $\mathbf{D}_{G(um)}$ are not comparable, the coherent multiple-wave interaction is weak (see Weckert & Hümmer, 1997). For example, for the cases considered in present paper, with weak primary reflection and strong secondary and coupling reflections, the $|\chi_G|$ of $\mathbf{D}_{G(2)}$ is much smaller than the $|\chi_{G-L}||\chi_L|$ of $\mathbf{D}_{G(um)}$ and the amplitudes of $\mathbf{D}_{G(2)}$ and $\mathbf{D}_{G(um)}$ usually are not comparable. To increase the multiple-wave interaction, *i.e.* phase sensitivity, the modulus of $\mathbf{D}_{G(um)}$ needs to be decreased by lowering the magnitude of the polarization vector $\mathbf{p}_{G(um)}(\mathbf{p}_O)$ so that the amplitudes of $\mathbf{D}_{G(um)}$ and $\mathbf{D}_{G(2)}$ are comparable. By a proper choice of the polarization $\mathbf{p}_O$ and the wavelength of the incident radiation, the magnitude of the polarization vector $\mathbf{p}_{G(um)}(\mathbf{p}_O)$ can be tailed to small values. Hence, the *Umweg* wave can be weakened or totally suppressed when the polarization factors $p_{um}^\sigma(\mathbf{p}_O)$ and $p_{um}^\pi(\mathbf{p}_O)$ of equation (3*b*) are close or equal to zero. For the total (exact) suppression, the following relation holds:

$$p_{um}^\sigma(\boldsymbol{\sigma}) p_{um}^\pi(\boldsymbol{\pi}_O) - p_{um}^\pi(\boldsymbol{\sigma}) p_{um}^\sigma(\boldsymbol{\pi}_O) = 0. \tag{7a}$$

This follows from equations (4*a*) and (4*b*) when the $p^{\sigma}_{um}(\mathbf{p}_O)$ and $p^{\pi}_{um}(\mathbf{p}_O)$ are simultaneously equal to zero. After consideration of all $\mathbf{s}$, $\boldsymbol{\sigma}$ and $\boldsymbol{\pi}$ vectors, for example, in the coordinate system ($\mathbf{s}_O$, $\boldsymbol{\sigma}$, $\boldsymbol{\pi}_O$), it can be easily verified that condition (7*a*) is equivalent to the condition

$$(\mathbf{s}_O \cdot \mathbf{s}_L)(\mathbf{s}_G \cdot \mathbf{s}_L) = 0. \qquad (7b)$$

To fulfil the condition of total suppression, the Bragg angle of either of the secondary L or the coupling $G - L$ reflections needs to be close or equal to 45°. Thus, the condition of total suppression can be fulfilled for two different wavelengths when the moduli of the diffracted vectors of the secondary and the coupling reflections (or the Bragg angles of these reflections) are different, and for one wavelength when the moduli of these vectors are the same. The polarization angle ω_s of the incident wave, *i.e.* $\omega = \omega_s$, that satisfies this condition is then equal to

$$\omega_s = -\arctan[p^{\sigma}_{um}(\boldsymbol{\sigma})/p^{\sigma}_{um}(\boldsymbol{\pi}_O)] \equiv -\arctan[p^{\pi}_{um}(\boldsymbol{\sigma})/p^{\pi}_{um}(\boldsymbol{\pi}_O)], \qquad (8)$$

which follows from equation (4*a*) or (4*b*).

Thus, the proposed weakening of the *Umweg* wave with strong secondary and coupling reflections by the decrease of the magnitude of the polarization vector $\mathbf{p}_{G(um)}(\mathbf{p}_O)$ can be considered as the polarization suppression of the *Umweg* wave.

2.2. Experimental

The experiments were carried out at the 1–9 keV bending-magnet beamline 15B of the Synchrotron Radiation Research Center (SRRC). The synchrotron storage ring was operating at 1.5 GeV and 200 mA. A newly constructed UHV-compatible six-circle soft X-ray diffractometer (Chen *et al.*, 1999) with κ geometry (Thorkildsen *et al.*, 1999, 2000) was used. A vacuum of 1.3×10^{-6} Pa was maintained to decrease the air absorption for X-rays with $\lambda = 1.762$ and 2.4108 Å. A semiconductor pin diode was used as the detector. Fig. 2 shows the experimental diffraction geometry that provides a variable polarization state of the incident radiation by changing the orientation of the crystal (through the χ, φ and κ circles of the diffractometer) relative to the polarized electric field (along the x axis) of the incident beam in the y direction. The z axis is along the vertical direction. The vector $\mathbf{G}_\sigma$ is normal to the diffraction plane of the G reflection. The angle between the x axis and $\mathbf{G}_\sigma$ is the polarization angle ω of the incident wave. The vertical and horizontal angular divergences of the beam after the double-crystal Si(111) monochromator and the collimation system were 0.010 and 0.025°, respectively. Multiple-wave diffractions were then performed by rotating (through the ψ circle of the diffractometer) the crystal around the **G** vector *via* the ψ scan. The detector could be moved along the 2θ and γ circles to monitor the diffracted waves. Fig. 3 shows the same parts of the multiple-wave ψ-scan diagrams for (i) π ($\omega = 90°$) and (ii) intermediate ($\omega = 65°$) polarization of the incident beam relative to the Si(222) symmetric Bragg primary reflection. The Miller indices of the secondary reflections and angles ω_s of polarization suppression are given in Fig. 3(*a*). The diffraction diagram (not shown) for the σ-polarized ($\omega = 0°$) incident beam is qualitatively the same as that shown in Fig. 3(*a*). The wavelength 1.762 Å of the incident radiation is selected so that the Bragg angle of the secondary 331 reflections is close to 45°. The background is the intensity of the primary reflection, 222. Fig. 3(*b*) shows appreciable suppression of the multiple-wave intensity for the peaks 331 and $\bar{3}3\bar{1}$ because the angles ω_s of polarization suppression coincide with the polarization angle ω of the incident wave ($\omega = \omega_s = 65°$). Fig. 3(*a*) shows the same intensities for the peaks located symmetrically with respect to the mirror point $\psi = 30°$, while Fig. 3(*b*) shows different intensities. This is in good agreement with equation

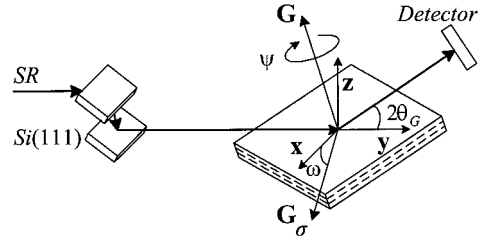

Figure 2
The diffraction geometry of the experiment.

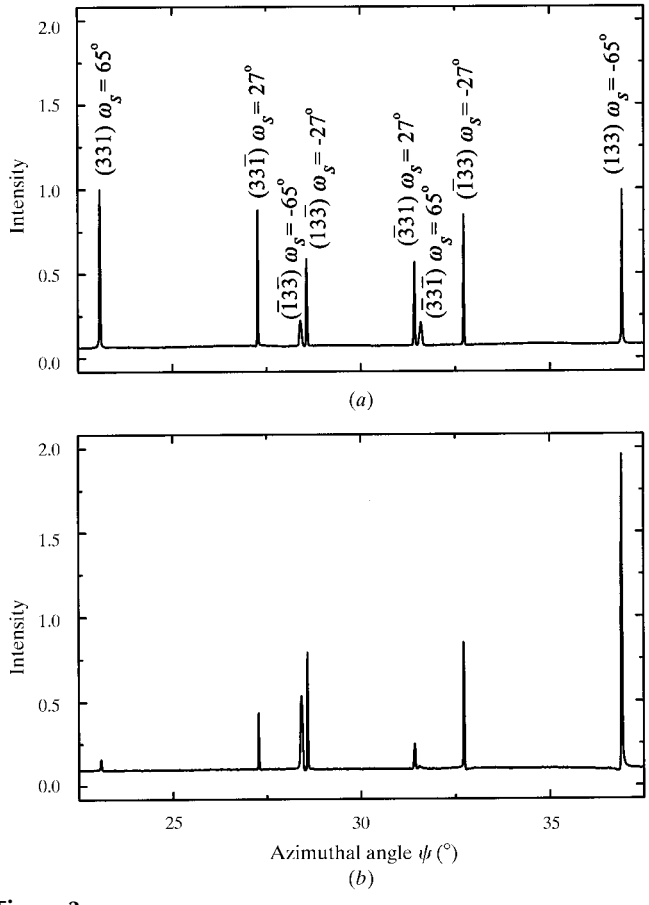

Figure 3
Multiple diffraction patterns of Si (222) and λ = 1.762 Å for (*a*) a π-polarized and (*b*) an intermediate (ω = 65°) polarized incident wave. Intensity is normalized with the maximaum intensity of the (331) peak of (*a*).

(2*b*). In particular, for the peak (133) with the angle $\omega_s = -65^\circ$ of polarization suppression far from the polarization angle $\omega = 65^\circ$ of the incident wave, intensity enhancement is also detected because the value of the length of the polarization vector $\mathbf{p}_{G(um)}(\mathbf{p}_O)$ of equation (2*b*) is larger for case (i) than for case (ii) (0.69 and 0.39, respectively).

3. Qualitative increase of the phase sensitivity

3.1. Theoretical consideration

The total suppression of $\mathbf{D}_{G(um)}$ fields is accompanied by the complete reduction of the phase sensitivity of multiple-wave diffraction. However, partial suppression of the $\mathbf{D}_{G(um)}$ field can provide comparable amplitudes of $\mathbf{D}_{G(um)}$ with $\mathbf{D}_{G(2)}$, thus increasing the phase sensitivity of the multiple-wave interaction. Such suppression can be realized in the following two ways: first, by using linearly polarized incident radiation with the polarization angle or/and wavelength rather close to the condition of exact suppression and, second, by using an elliptically polarized incident beam of synchrotron radiation with a rather small value of the ellipticity parameter b_e when the main linearly polarized component of this beam is under the condition of exact suppression.

Consider the general case of elliptically polarized incident radiation, in which the polarization vector can be represented as

$$\mathbf{p}'_O = (\alpha - ib_e\beta)\boldsymbol{\sigma} + (\beta + ib_e\alpha)\boldsymbol{\pi}_O \equiv \mathbf{p}_O + ib_e\mathbf{p}_O^{\perp},$$

where $\mathbf{p}_O$ is the main linear component of an elliptically polarized radiation and vector $\mathbf{p}_O^{\perp}$ is normal to $\mathbf{p}_O$. α and β in equations (3*a*), (4*a*) and (4*b*) are replaced now by $\alpha - ib\beta$ and $\beta + ib_e\alpha$, respectively. Following the derivations of the papers of Chang & Tang (1988) and Chang *et al.* (1989) for second-order Born approximation, the relative intensity $I_{G(3)}/I_{G(2)} = \mathbf{D}_{G(3)}\mathbf{D}^*_{G(3)}/(\mathbf{D}_{G(2)}\mathbf{D}^*_{G(2)})$ *versus* the reduced azimuthal angle parameter $\varphi = 2\Delta\psi/\eta$ can be expressed as

$$I_{G(3)}/I_{G(2)} = 1 + A^{-1}F\{B[\varphi\cos(\delta_3 - \delta_e) - \sin(\delta_3 - \delta_e)] + FC\} \times (\varphi^2 + 1)^{-1}, \quad (9)$$

where $\eta = |\chi_O|/(\boldsymbol{\sigma}\cdot\mathbf{s}_L)\cos\theta_G$ is the fundamental width (see Chang *et al.*, 1989) of the three-wave diffraction, δ_3 is the triplet phase of the structure-factor triplet $F_L F_{G-L}/F_G$,

$$\delta_e = \arctan(B_1/B_2) \quad (10)$$

is an elliptical phase shift and

$$F = |F_{G-L}|\,|F_L|/(|F_O|\,|F_G|)$$
$$A = a_\sigma^2 + a_\pi^2 + b_e^2(b_\sigma^2 + b_\pi^2)$$
$$C = c_\sigma^2 + c_\pi^2 + b_e^2(d_\sigma^2 + d_\pi^2)$$
$$B = (B_1^2 + B_2^2)^{1/2}$$
$$B_1 = b_e(a_\sigma d_\sigma + a_\pi d_\pi - b_\sigma c_\sigma - b_\pi c_\pi)$$
$$B_2 = a_\sigma c_\sigma + a_\pi c_\pi + b_e^2(b_\sigma d_\sigma + b_\pi d_\pi)$$
$$a_\sigma = \alpha P_G^\sigma, \quad a_\pi = \beta P_G^\pi, \quad b_\sigma = -\beta P_G^\sigma, \quad b_\pi = \alpha P_G^\pi$$
$$c_s \equiv p^s_{um}(\mathbf{p}_O), \quad d_s = -\beta p^s_{um}(\boldsymbol{\sigma}) + \alpha p^s_{um}(\boldsymbol{\pi}_O), \quad s \equiv \sigma \text{ or } \pi.$$

Thus, the use of an elliptically polarized incident beam introduces the elliptical phase shift δ_e (see also Shen & Finkelstein, 1990). Far from the suppression condition of the main component $\mathbf{p}_O$ ($|c_\sigma| > 0$ or/and $|c_\pi| > 0$), $\delta_e \to 0^\circ$ when $b_e \to 0$ while, under the condition $c_\sigma = c_\pi = 0$, $\delta_e \to 90^\circ$ when $b_e \to 0$.

As follows from equation (9), for high phase sensitivity (see also Weckert & Hümmer, 1997), the value of B has to be comparable with FC and greater than FC, *i.e.* the parameter

$$S \equiv FC/B \leq 1. \quad (11)$$

For conventional three-wave cases (far from the suppression condition) involving a weak primary reflection and strong secondary and coupling reflection, the value of FC is much larger than B ($S \gg 1$). These cases are of low phase sensitivity owing to the large value of the phase-independent component (see Chang & Tang, 1988; Chang *et al.*, 1989). On the other hand, for the cases close to the suppression condition and the linearly ($b_e = 0$) polarized incident radiation, the values S, FC and B are close to zero. These cases are also of low phase sensitivity owing to the low visibility of the three-wave peak profiles on the background of the two-wave intensity. The partial suppression of the *Umweg* wave can realize the inter-

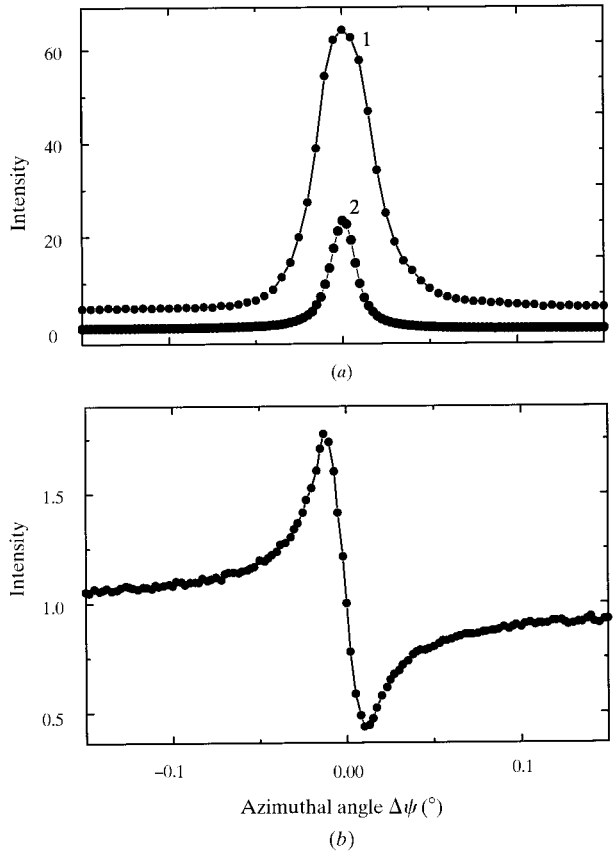

Figure 4
Intensity profiles of GaAs three-wave (000, 222, 311) diffraction and λ = 2.4108 Å for (*a*) σ (curve 1), π (curve 2) and (*b*) intermediate (ω = 47°) polarization state of the elliptically polarized (b_e = 0.15) incident wave. Intensity is normalized with the two-wave (222) intensity of (*b*). The difference in intensity and peak width of curves 1 and 2 is due to the beam divergences.

mediate situations in which the value $S \leq 1$. Thus, in comparison with the two previous cases, the qualitative increase of the phase sensitivity of the three-wave peak profiles is achieved.

3.2. Experimental and dynamical calculations

The above-mentioned qualitative increase of the phase sensitivity is verified experimentally for the model crystal GaAs with well known structure. The (000; 222; 311) three-wave diffraction with a weak primary reflection (222) and strong secondary (311) and coupling ($\bar{1}11$) reflections is investigated. The wavelength 2.4108 Å of the incident radiation is selected so that the Bragg angle of the secondary (311) reflection is close to 45° and the polarization suppression of the *Umweg* wave at the polarization angle $\omega = 47°$ is fulfilled. Fig. 4 shows the experimental peak profiles for (i) σ (curve 1), π (curve 2) and (ii) intermediate ($\omega = 47°$) polarization states of the elliptically polarized incident beam with the ellipticity parameter $b_e = 0.15$. Here, the polarization state of the elliptically polarized beam means the polarization of the linear component $\mathbf{p}_O$. The value of the ellipticity parameter was estimated by the conventional method used in the synchrotron-radiation facility and that proposed by Shen & Finkelstein (1990). The positive direction of the azimuthal rotation $\Delta\psi$ in Fig. 4, the same as in Figs. 5–7, corresponds to the movement of the reciprocal-lattice point of the secondary reflection L towards the Ewald sphere. This direction is experimentally determined by the method described, in particular, by Stetsko & Chang (1999*b*). The parameter b_e is so chosen that $S = 0.86$ for case (ii) to satisfy the condition for high phase sensitivity. Accordingly, $S = 2.9$ for the σ polarization state and $S = 18$ for the π polarization state of the incident beam. For comparison, Figs. 5–7 show the peak profiles calculated for artificially assigned values (Weckert & Hümmer, 1997; Stetsko & Chang, 1999*a*,*b*) of the triplet phase δ_3 for cases of different S values using the dynamical theory without approximation (Stetsko & Chang, 1997). Some overlapped curves, such as curve 4 in Fig. 5(*b*) and curves 1 and 3 in Fig. 7(*a*), are shown but not numbered. The lowest phase sensitivity is observed in Fig. 5(*b*) for π polarization when S is much greater than 1. The curves calculated for $\delta_3 = -90, 0, 90$ and 180° are practically indistinguishable. Slightly higher sensitivity with S approximately equal to 3 is detected for σ polarization (Fig. 5*a*) and the highest sensitivity with $S \leq 1$ is shown in Fig. 6, where the partial suppression of the *Umweg* wave is realized. Fig. 6 shows the well known shapes of the peak profiles for the high phase sensitivity case. The peak profiles calculated for $\delta_3 = -90$ and 90° (curves 1 and 3, respectively) are asymmetric with comparable large maximum and minimum intensity deviations from the intensity of the two-wave case. The peak profiles calculated for $\delta_3 = 0$ and 180° are practically symmetric with different extreme intensity deviation (maximum for curve 2 and minimum for curve 4, respectively) from the intensity of the two-wave case. Similar to Fig. 5(*b*), Fig. 7(*a*) also shows negligibly low phase sensitivity ($S = 0$) of the profiles for the linearly polarized ($b_e = 0$) incident radiation at the exact polarization-suppression condition. It should be noted that Fig. 7(*a*) shows the well known *Aufhellung* phenomenon (Wagner, 1923), which cannot be explained by the second-order Born approximation used in this paper.

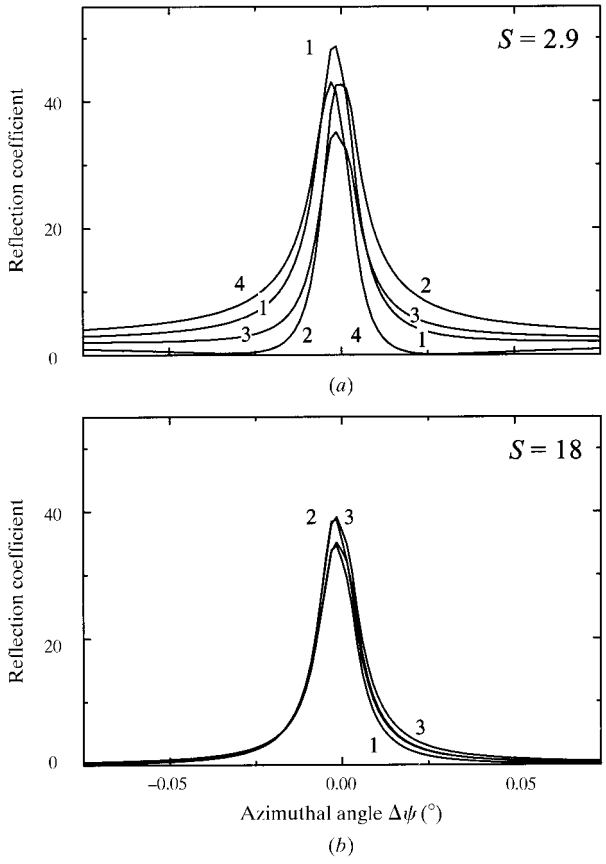

Figure 5
Calculated profiles of Fig. 4 for (*a*) σ and (*b*) π polarization states of the elliptically polarized (b_e = 0.15) incident wave. Curves 1, 2, 3 and 4 correspond to δ_3 = −90, 0, 90 and 180°, respectively. Intensity is normalized with the two-wave (222) intensity of Fig. 6.

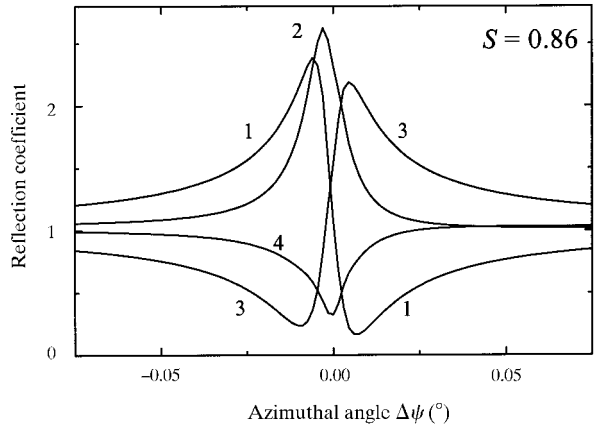

Figure 6
Calculated profiles for intermediate (ω = 47°) polarization state of the elliptically polarized (b_e = 0.15) incident wave. Curves 1, 2, 3 and 4 correspond to δ_3 = −90, 0, 90 and 180°, respectively. Intensity is normalized with the two-wave (222) intensity.

From the comparison of the experimental curve shown in Fig. 4(*b*) with curve 1 of Fig. 6, the value of δ_3 for GaAs (000; 222; 311) is estimated to be about -90°, compared to the theoretical value $\delta_3 = -95^\circ$ calculated from the known structure. For the curves of Fig. 6, the value of the elliptical phase shift δ_e of equation (10) is about 81°. Therefore, these curves show the well known phase-dependent distributions (see, for example, Weckert & Hümmer, 1997; Chang, 1998) with respect to the value of $\delta_3 - \delta_e$. For example, the $\delta_3 - \delta_e$ value is about -180° for curve 1. Thus, when the main linear component $\mathbf{p}_O$ of the elliptically polarized incident beam is under the condition of exact suppression, the weak linear component $ib_e\mathbf{p}_O^{\perp}$ of the incident beam with the shifted value of $\delta_3 - \delta_e$ produces the experimentally obtained asymmetric profile (Fig. 4*b*).

As mentioned above, the partial polarization suppression can also be realized by using linearly polarized incident ($b_e = 0$) radiation with the polarization angle and/or wavelength close to the condition of exact suppression. Experimentally, using radiation from wigglers or the exact electron-orbital plane of bending magnets can fulfil this condition. Theoretically, dynamical calculations also demonstrate the possibility of the realization of this partial polarization suppression for increasing the phase sensitivity. For example, Fig. 7(*b*) shows the peak profiles calculated for the case of the linearly polarized incident radiation with the polarization angle $\omega = 40^\circ$ rather close to the angle of exact suppression. The high phase sensitivity ($S = 0.62$) of the profiles is observed. The absence of the elliptical phase shift ($\delta_e = 0$) leads to the conventional phase dependence of the shapes of the three-wave peak profiles. This well known phase dependence is characterized by asymmetric peak profiles for $\delta_3 = 0^\circ$ and $\delta_3 = 180^\circ$ and practically symmetric peak profiles for $\delta_3 = -90$ and 90°. In particular, the profile of curve 1 corresponding to $\delta_3 = -90^\circ$ is expected to occur for the GaAs three-wave case using linearly polarized incident radiation.

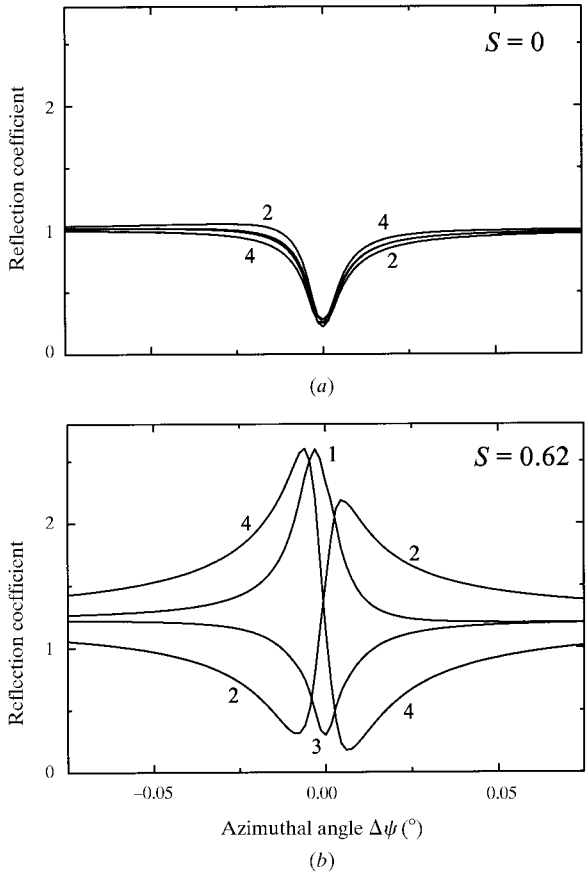

Figure 7
Calculated profiles for intermediate (*a*) ω = 47° and (*b*) ω = 40° polarization of a linearly polarized (b_e = 0) incident wave. Curves 1, 2, 3 and 4 correspond to δ_3 = −90, 0, 90 and 180°, respectively. Intensity is normalized with the two-wave (222) intensity of Fig. 6.

In view of the fact that the above polarization suppression can be realized for the pre-selected wavelength, the applicability of the proposed method is limited by the range of accessible wavelengths of the synchrotron radiation. Nevertheless, this method practically can be used for the wide class of real crystals. For example, for crystals with a large unit cell, such as the macromolecular crystal of tetragonal lysozyme (see Weckert & Hümmer, 1997; Chang, Chao *et al.*, 1999), and conventional X-ray wavelengths, the condition of polarization suppression of the comparatively strong *Umweg* wave can be, in principle, realized for a large number of the three-wave cases. In particular, for Cu $K\alpha_1$ incident radiation and the three-wave diffraction (000; 115; 50,50,$\bar{8}$) for lysozyme (Protein Data Bank No. 1LYZ), the primary reflection (115) is rather weak ($|F_G| = 128$), while the secondary (50,50,$\bar{8}$) and the coupling ($\overline{49}$,$\overline{49}$,13) reflections are comparably strong ($|F_L| = 462$ and $|F_{G-L}| = 562$, respectively). The Bragg angle of the secondary reflection is close to 45°, while the Bragg angle $\theta_G = 5.9^\circ$ of the primary reflection is rather small. Hence, the primary reflection can be detected as usual for macromolecules. Under this condition, the polarization suppression of the *Umweg* wave can be achieved at $\omega_s = -14^\circ$.

In conclusion, we have observed a new phenomenon of polarization suppression of the multiple-wave X-ray interaction in crystals owing to the suppression of the intensity of the *Umweg* multiple waves. Based on this, a method to qualitatively increase the phase sensitivity in multiple-wave diffraction using an elliptically or a linearly polarized radiation under partial polarization suppression conditions has been realized. This method thus provides a new way of using multiple-wave diffraction for effectively determining the X-ray reflection phases.

The authors are indebted to the National Science Council for financial support. YPS, YSH, CHC and CKC are very grateful to the same organization for providing a visiting scholarship and graduate fellowships during the course of this study.

References

Chang, S. L. (1984). *Multiple Diffraction of X-rays in Crystals.* Heidelberg: Springer-Verlag.

Chang, S. L. (1987). *Crystallogr. Rev.* **1**, 87–189.
Chang, S. L. (1998). *Acta Cryst.* A**54**, 886–894.
Chang, S. L., Chao, C. H., Huang, Y. S., Jean, Y. C., Sheu, H. S., Liang, F. J., Chien, H. C., Chen, C. K. & Yuan, H. S. (1999). *Acta Cryst.* A**55**, 933–938.
Chang, S. L., Huang, M. T., Tang, M. T. & Lee, C. H. (1989). *Acta Cryst.* A**45**, 870–878.
Chang, S. L., Stetsko, Yu. P., Huang, Y. S., Chao, C. H., Liang, F. J. & Chen, C. K. (1999). *Phys. Lett. A*, **264**, 328–333.
Chang, S. L. & Tang, M. T. (1988). *Acta Cryst.* A**44**, 1065–1072.
Chen, C. K., Chung, C. H., Shu, C. H., Lee, Y. R. & Chang, S. L. (1999). XVIIIth IUCr Congress, Glasgow, Scotland, Abstract P12.01.009.
Colella, R. (1974). *Acta Cryst.* A**30**, 413–423.
Hauptman, H. A. (1989). *Phys. Today*, **42** (November), 24–29.
Hendrickson, W. A. (1991). *Science*, **254**, 51–58.
Høier, R. & Marthinsen, K. (1983). *Acta Cryst.* A**39**, 854–860.
Hümmer, K. & Billy, H. W. (1986). *Acta Cryst.* A**42** 127–133.
Juretschke, H. J. (1982*a*). *Phys. Rev. Lett.* **48**, 1487–1489.
Juretschke, H. J. (1982*b*). *Phys. Lett.* **92**A, 183–185.
Juretschke, H. J. (1984). *Acta Cryst.* A**40**, 379–389.
Juretschke, H. J. (1998). *Cryst. Res. Technol.* **33**, 569–581.
Larsen, H. B. & Thorkildsen, G. (1998). *Acta Cryst.* A**54**, 129–136.
Renninger, M. (1937). *Z. Kristallogr.* **97**, 107–121.
Schenk, H. (1991). Editor. *Direct Methods for Solving Crystal Structures.* New York: Plenum Press.
Shen, Q. (1986). *Acta Cryst.* A**42**, 525–533.
Shen, Q. (1998). *Phys. Rev. Lett.* **80**, 3268–3271.
Shen, Q. & Colella, R. (1988). *Acta Cryst.* A**44**, 17–21.
Shen, Q. & Finkelstein, K. D. (1990). *Phys. Rev. Lett.* **65**, 3337–3340.
Shen, Q. & Finkelstein, K. D. (1992). *Phys. Rev. B*, **45**, 5075–5078.
Shen, Q., Shastri, S. & Finkelstein, K. D. (1995). *Rev. Sci. Instrum.* **66**, 1610–1613.
Stetsko, Yu. P. & Chang, S. L. (1997). *Acta Cryst.* A**53**, 28–34.
Stetsko, Yu. P. & Chang, S. L. (1999*a*). *Acta Cryst.* A**55**, 457–465.
Stetsko, Yu. P. & Chang, S. L. (1999*b*). *Acta Cryst.* A**55**, 683–694.
Thorkildsen, G. (1987). *Acta Cryst.* A**43**, 361–369.
Thorkildsen, G. & Larsen, H. B. (1998). *Acta Cryst.* A**54**, 120–128.
Thorkildsen, G., Larsen, H. B., Mathiesen, R. H. & Mo, F. (2000). *J. Appl. Cryst.* **33**, 49–51.
Thorkildsen, G., Mathiesen, R. H. & Larsen, H. B. (1999). *J. Appl. Cryst.* **32**, 943–950.
Wagner, E. (1923). *Phys. Z.* **21**, 94–98.
Weckert, E. & Hümmer, K. (1997). *Acta Cryst.* A**53**, 108–143.
Woolfson, M. M. & Fan, H. F. (1995). *Physical and Non-physical Methods of Solving Crystal Structures.* Cambridge University Press.